Keratin Expression Provides Novel Insight into the Morphogenesis and Function of the Companion Layer in Hair Follicles

Li-Hong Gu[1] and Pierre A. Coulombe[1]

Hair follicles cycle between stages of growth (anagen) and metabolic quiescence (telogen) throughout life. In mature follicles, transition from telogen back into anagen involves the activation, proliferation, and differentiation of epithelial stem cells located in the bulge, a specialization of the outer root sheath. Recent studies identified keratin 6a (*K6a*) transcripts as enriched in bulge epithelial stem cells in mouse skin. We used messenger RNA probes, antibodies, a LacZ reporter mouse model, and whole-mount staining assays to investigate the regulation of *mK6a* during mouse postnatal hair cycling, and compare it to *mK75*, a companion layer (Cl) marker. We find that *mK75* regulation parallels that of inner root sheath (IRS) markers, with expression onset at anagen IIIa above the new hair bulb and subsequent spreading towards the bulge. Although also occurring in the Cl, *mK6a* expression begins at anagen IIIb in differentiating cells located proximal to the bulge, and subsequently spreads towards the hair bulb. *mK6a* and *mK75* thus exhibit temporally distinct, and spatially opposed, expression patterns in the Cl during postnatal anagen. These findings provide novel insight into the morphogenesis and properties of the Cl, and raise the distinct possibility that it is an integral part of the IRS compartment.

Journal of Investigative Dermatology (2007) **127,** 1061–1073. doi:10.1038/sj.jid.5700673; published online 14 December 2006

INTRODUCTION

Epithelial appendages, including hair, nail, glands, tooth, etc., are topologically complex miniature organs that develop from the single-layered ectoderm during embryogenesis (Hardy, 1992). Mature hair follicles, in particular, comprise eight epithelial layers, each the product of a distinct terminal differentiation pathway, organized in concentric circles around the main axis of the follicle. They are, from inside out, the medulla, cortex, and cuticle, which form the hair shaft; another cuticle, the Huxley's and Henle's layers (He), which form the inner root sheath (IRS); the companion layer (Cl), and finally, the outer root sheath (ORS), a stratified epithelium that wraps around the follicle and is contiguous with the epidermis. The various types of hair follicles occurring in mammals share the same general architecture (Hardy, 1992; Sundberg and Hogan, 1994).

A fascinating property of hair follicles is the unique developmental cycle they undergo throughout life, with phases of rapid growth (anagen) interspersed with involution (catagen) and rest (telogen) (Hardy, 1992). This cycle recapitulates many of the key events occurring during morphogenesis, and requires the temporal and spatial integration of multiple stimulatory and inhibitory signals (Paus and Cotsarelis, 1999; Fuchs *et al.*, 2001; Millar, 2002). Growth of a new hair requires re-entry into anagen via the activation of progenitor (stem) cells residing in, or near, a specialized part of the follicle ORS known as the bulge (Cotsarelis *et al.*, 1990; Taylor *et al.*, 2000; Oshima *et al.*, 2001). Activating signals that emanate from mesenchymal cells located in the proximal dermal papilla direct progenitor cells to divide rapidly, migrate downward, and differentiate to regenerate a hair bulb, from which a new hair shaft will emerge (Cotsarelis *et al.*, 1990; Taylor *et al.*, 2000; Oshima *et al.*, 2001; Alonso and Fuchs, 2003). In specific settings, for example, after skin epithelial injury, bulge epithelial cells also participate in epidermal homeostasis (Ito *et al.*, 2005; Levy *et al.*, 2005). Also, non-melanoma skin tumors often originate from progenitor cells housed in hair follicles (Stenback, 1980; Morris *et al.*, 1986; Hutchin *et al.*, 2005; Cotsarelis, 2006). Not surprisingly, therefore, there has been considerable interest in hair follicles, and its fascinating growth cycle, in recent years.

A single layer of flattened epithelial cells, the Cl, occurs between the outer and IRS compartments of hair follicles. This layer was initially recognized as being distinct from the ORS based on electron microscopy observations (Ito, 1986, 1988). A growing list of molecular markers, starting with

[1]*Departments of Biological Chemistry and Dermatology, The Johns Hopkins University School of Medicine, Baltimore, Maryland, USA*

Correspondence: Dr Pierre A. Coulombe, Department of Biological Chemistry, Johns Hopkins University School of Medicine, 725 N. Wolfe Street, Baltimore, Maryland 21205, USA. E-mail: coulombe@jhmi.edu

Abbreviations: Cl, companion layer; He, Henle layer; IRS, inner root sheath; mRNA, messenger RNA; ORS, outer root sheath; PBS, phosphate-saline buffer

Received 24 July 2006; revised 22 October 2006; accepted 23 October 2006; published online 14 December 2006

keratin 6hf (now renamed as K75; Winter *et al.*, 1998; Wojcik *et al.*, 2001; Schweizer *et al.*, 2006) and now including the serpin plasminogen activator inhibitor type 2 (PAI-2) (Jensen *et al.*, 2000), microtubule associated protein-2 (Hallman *et al.*, 2002) and calretinin (Poblet *et al.*, 2005), confirmed that the program of differentiation giving rise to the Cl is distinct from the ORS and IRS layers. Yet, the function of the Cl and its relationship to the proximal ORS and IRS has remained incompletely understood.

Given their large number (>50) and differentially regulated expression, keratins are very useful as markers reflecting the type and differentiated state of epithelial cells, including those making up hair follicles. Several years ago, researchers provided evidence that K15 and K19 antigens occur at higher levels in hair bulge epithelial cells *in vivo* (Michel *et al.*, 1996; Lyle *et al.*, 1998; Liu *et al.*, 2003). More recently, several researchers reported on the isolation and characterization of hair bulge-derived cells that are highly enriched in epithelial stem cells. In two such studies involving mouse skin, gene expression profiling suggested that the messenger RNA (mRNA) for the type II keratin 6a (K6a) paralog occurs at higher levels in bulge epithelial cells compared to epidermal basal cells, chosen as a reference (Tumbar *et al.*, 2004; Morris *et al.*, 2004). In a third study, also carried out in the mouse, K6 immunoreactivity was seen to coincide with CD34, a cell surface marker reported to be enriched in the hair bulge epithelial stem cells (Trempus *et al.*, 2003). Before these reports, K6 antigens and/or mRNAs had been localized to the ORS (Takahashi *et al.*, 1998) and, specifically, to the Cl in anagen-stage hair follicles (e.g., Rothnagel and Roop, 1995; Winter *et al.*, 1998; Rothnagel *et al.*, 1999; Wojcik *et al.*, 2001; Bernot *et al.*, 2002). In telogen-stage follicles, K6 immunoreactivity occurs in the club hair sheath (Bernot *et al.*, 2002), a multilayered epithelium wrapping around the base of the club hair, featuring cells anchoring the hair on its inner side and progenitor cells giving rise to the next generation of anagen hairs on its outer side (Wilson *et al.*, 1994; Koch *et al.*, 1998). The status of *mK6a* as a marker enriched in epithelial stem cells located in the bulge thus remains unclear.

Here, we analyzed the regulation of *mK6a* mRNA during hair follicle cycling. We used *in situ* hybridization for the *mK6a* mRNA as well as a previously described *hK6a*-LacZ transgenic mouse model (Takahashi and Coulombe, 1996, 1997) to circumvent specificity problems related to the high homology between K6a and related type II keratins (Wang *et al.*, 2003), as well as sensitivity problems related to keratin epitope modifications in hair follicle tissue (Nachat *et al.*, 2005). These studies were conducted in whole-mount preparations of mouse tail skin (Braun *et al.*, 2003), in which the hair follicles are not only larger but histological sectioning plane effects are reduced. Finally, we related our *mK6a* findings to those of *mK75*, a bonafide marker of the Cl (Winter *et al.*, 1998; Wojcik *et al.*, 2001; Wang *et al.*, 2003) (see comment about keratin gene nomenclature under ''Materials and Methods''), and trichohyalin, which is expressed in the IRS and hair medulla (O'Guin *et al.*, 1992). We find that *mK6a* exhibit a novel and unique regulatory pattern during hair cycling, which is restricted to the Cl and proceeds in a hair bulge to hair bulb direction. This pattern is temporally and spatially distinct from that of *mK75*, which closely parallels that of trichohyalin in the IRS. Our findings also suggest that very few *mK6a*-expressing cells are actively dividing, and none appears to be ''slow-cycling'', a typifying feature of stem cells. The significance of the *mK6a* and *mK75* mRNA patterns for the morphogenesis and properties of the Cl, and its relationship to the outer and IRS compartments in hair follicles, are discussed.

RESULTS

mK6a mRNA distribution during hair follicle cycling

We examined the distribution of *mK6a* mRNA during the first postnatal hair follicle cycle using *in situ* hybridization. Mouse tail skin epithelial preparations, which are ideally suited for whole-mount labeling procedures (Braun *et al.*, 2003), were hybridized with a probe specific for the *mK6a* mRNA (Takahashi *et al.*, 1998). Pilosebaceous units (i.e., a hair follicle with a pair of sebaceous glands) are organized in triads in mouse tail skin, with the middle hair follicle cycling ahead of the flanking ones (Schweizer and Marks, 1977). Otherwise, hair cycling occurs exactly as in pelage skin (Gu and Coulombe, unpublished data), and thus the morphological criteria defined by Muller-Rover *et al.* (2001) could be applied to stage tail follicles along their postnatal cycle. Tissue sampling was conducted between P22, when tail skin follicles are in telogen, to the next telogen at P55.

During telogen, the *mK6a* mRNA was detected in the innermost layer of the club sheath, forming a cup around the club hair proper (Figure 1a). The epithelial downgrowth that initially forms following the onset of anagen is negative for the *mK6a* mRNA (Figure 1b and c). Starting at anagen IIIb and established by stage IIIc, the *mK6a* mRNA occurs near the base of the telogen follicles (Figure 1d and e), and progressively extends downward between late anagen IIIc and VI (Figure 1f–i). Additional data reported below confirms these assignments. Once follicles are maximally elongated (anagen V–VI), the hybridization signal reaches down to the suprabulbar region of the follicle (Figure 1h and i). During that period, the signal for *mK6a* mRNA persists in the club hair sheath of the previous follicle until anagen VI (Figure 1e–i). By mid and late catagen (Figure 1j–l), the signal for *mK6a* becomes significantly stronger in the narrower follicular base, forming a ''filled cup'' that persists as the follicle completes its regression. The newly formed telogen hair follicle exhibits a hybridization pattern identical to that shown in Figure 1a (data not shown). A sense probe yielded background staining (Figure 1m), establishing specificity.

mK6a regulation is reproduced by the human K6a gene promoter in transgenic reporter mice

We previously reported on a *hK6a-LacZ* mouse model (Takahashi and Coulombe, 1996, 1997) in which 5.2 kb of 5′ upstream sequence from the cloned human *K6a* gene (Takahashi *et al.*, 1995) controls the expression of a *LacZ* reporter modified with a nuclear localization signal. As described then, conventional pre-embedding X-gal staining

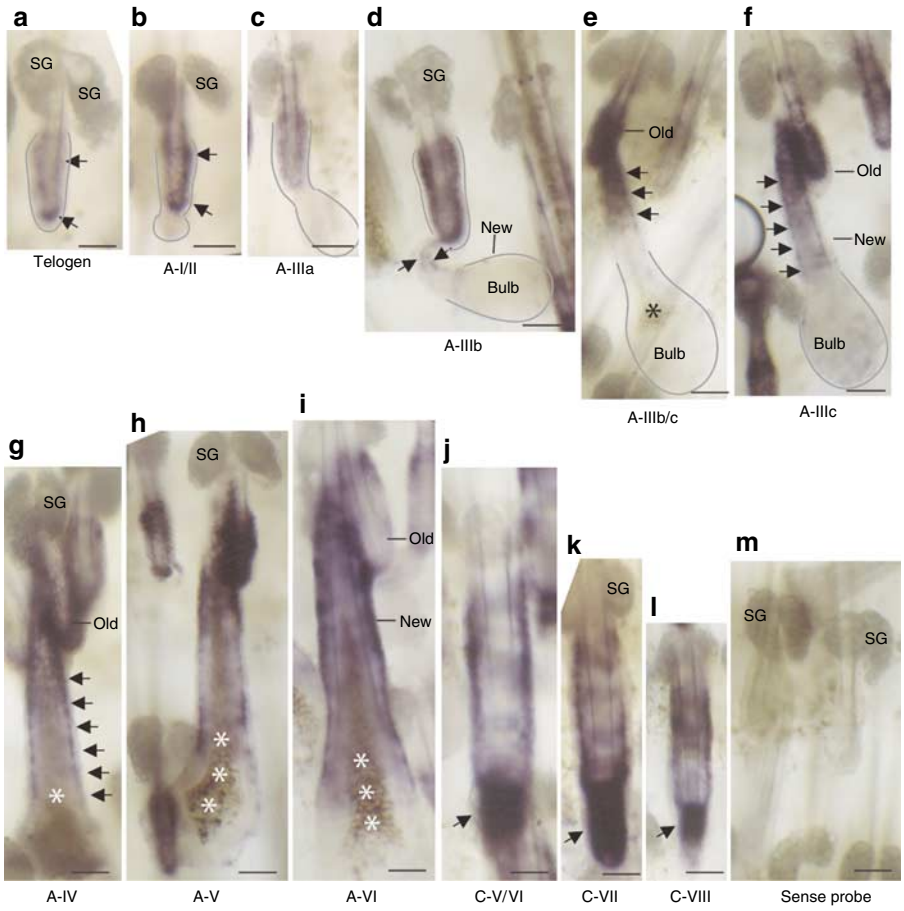

Figure 1. Regulation of endogenous *mK6a* mRNA during postnatal hair follicle cycling in mouse. Whole-mount tail epidermal sheets, prepared from P22-P55 wild-type mice, were hybridized with (**a–l**) antisense and (**m**) sense probes specific for the *mK6a* mRNA. Representative results are shown. Hair cycle stage is indicated below each micrograph. In frames (**a–f**), a line depicts the outer limit of relevant areas of follicular tissue. Positive hybridization was detected in the innermost epithelial layer of the bulge during telogen (**a**; see arrows). This distribution was maintained in anagen I/II (**b**; see arrows) and (**c**) anagen IIIa. (**d**) At anagen IIIb, additional hybridization appears in the newly formed hair (''new''), proximal to the club hair sheath (see opposing arrows in **d**). Thereafter, the signal intensifies and spreads downward, in the direction of the maturing hair bulb, during (**e**) anagen IIIb/c, (**f**) anagen IIIc, (**g**) anagen IV, (**h**) anagen V, and (**i**) anagen VI. (**i**) During that period, a strong signal for the *mK6a* mRNA is maintained in the club hair sheath of the previous hair (''old'') until anagen VI, at which time it has disappeared (**i**). (**j–l**) During catagen, the signal for *mK6a* becomes stronger but restricted to the narrowing base of the involuting follicle. (**m**) The sense probe yielded background staining in these preparations. SG, sebaceous gland; bulb, hair bulb. Asterisks depict melanin pigmentation that should not be confused with hybridization signal. Bar = 50 μm.

failed to detect significant LacZ expression in anagen-stage pelage hair follicles in these mice. In contrast, LacZ activity could be readily detected in the larger vibrissae follicles (Takahashi and Coulombe, 1997) and at the edge of skin wounds, which are less prone to sectioning plane effects. Wishing to extend the analysis of *K6a* expression during hair follicle cycling, we performed whole-mount X-gal stainings as well as LacZ antibody stainings on tail skin preparations from *hK6a-LacZ* mice.

During telogen, the lacZ reporter is expressed predominantly in two locations: near the base of the club hair, and in particular, in a ring structure slightly below the sebaceous glands (Figure 2a and b). As was the case for *mK6a* mRNA, the outer epithelial layer surrounding the club hair is devoid of signal (Figure 2a and b). This distribution is maintained (Figure 2c, d) until anagen stage IIIb, at which time a small group of nuclei apposed against the club hair base now express LacZ (Figure 2e and f). Although the number of Lac-Z-positive nuclei has increased by anagen stage IIIc/IV, reporter activity remains proximal to the old club hair sheath so that the bulk of the epithelial downgrowth that has formed below is conspicuously devoid of activity (Figure 2g, h). As anagen progresses further to stages V (Figure 2i and j) and VI (data not shown), expression of LacZ spreads in a downward direction but, as is the case for *mK6a*, does not reach beyond the suprabulbar region. By mid-catagen, LacZ expression has reorganized into a cylinder capped at the distal (bulb) end (Figure 2k and l). As the follicle progresses to late catagen, the lacZ expression domain shortens whereas the signal increases in intensity (e.g., Figure 2m and n). This process continues until the pattern characteristic of telogen is re-achieved (data not shown; see Figure 2a). This pattern, which was observed in two independent lines of *hK6a*-LacZ mice, thus closely mimics that of the endogenous *mK6a* mRNA (Figure 1).

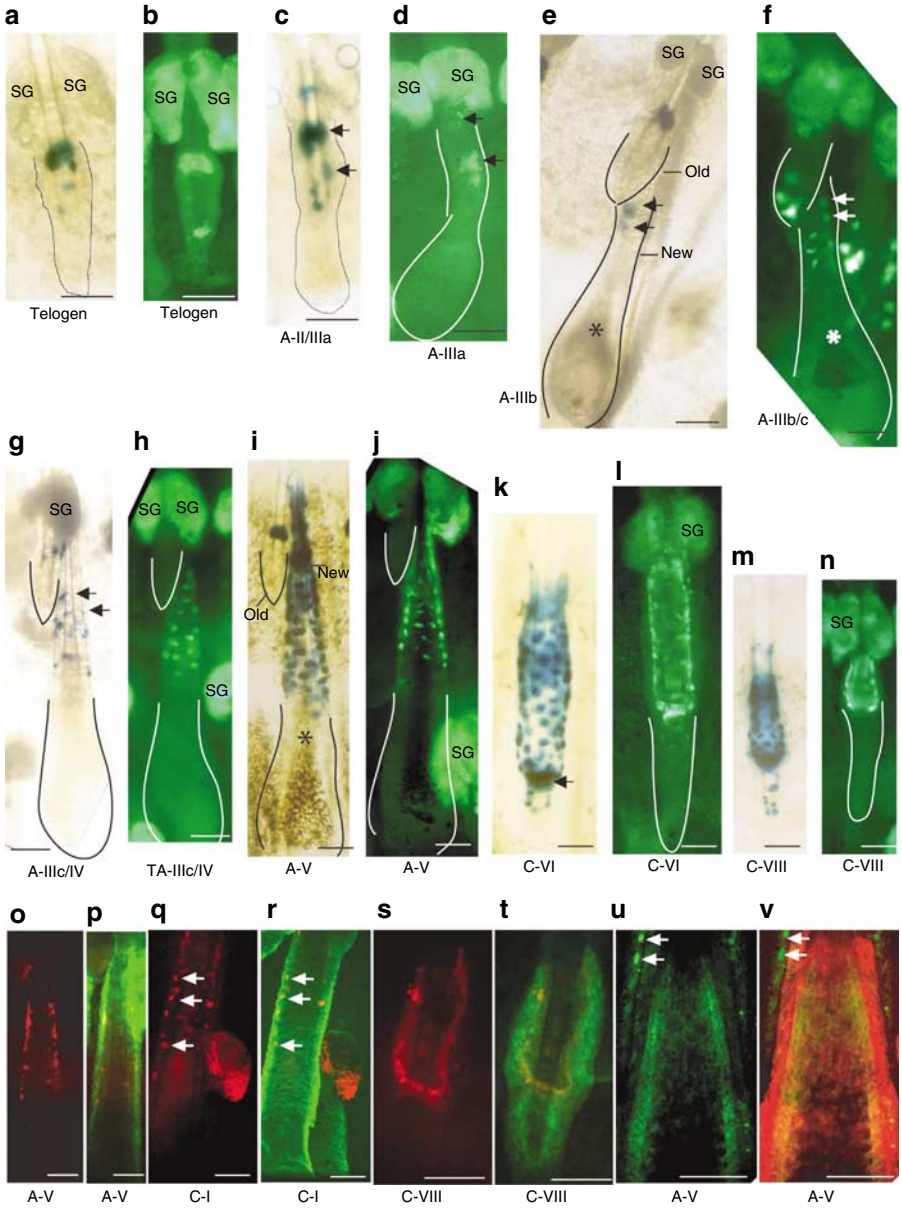

Figure 2. Regulation of *hK6a*-LacZ reporter during postnatal hair follicle cycling in transgenic mice. (**a**–**n**) Whole-mount tail epidermal sheets, prepared from P22-P55 *hK6a*-LacZ transgenic mice, were processed for X-gal staining, to detect LacZ enzymatic activity, or LacZ antibody, to detect the corresponding antigen. Representative results are shown. Hair cycle stage is indicated below each micrograph. In frames, lines depict the outer limits of the relevant areas of the club hair sheath of the previous hair (''old'') and/or newly formed hair (''new''). The LacZ open reading frame contains a nuclear localization signal.
All incubations in X-gal staining solutions were carried out for 1 hour. (**a**, **b**) During telogen and early anagen (II/IIIa; see **c**, **d**), LacZ-positive cells occur near the base of the club hair and in a ring-like structure below the sebaceous glands (see arrows). (**e**, **f**) By anagen IIIb, at which time the tip of the newly emerging hair nears the club hair sheath of the old one, a small group of nuclei apposed to the club hair base express LacZ (arrows). (**e**–**j**) Subsequently (anagen IIIc->V), LacZ expression intensifies and progressively spreads in the direction of the bulb. (**k**–**n**) During catagen, the signal for *mK6a*-LacZ becomes stronger but restricted to the narrowing base of the involuting follicles. No signal occurs in similar preparations from non-transgenic mice (data not shown). SG, sebaceous gland; bulb, hair bulb. Asterisks depict melanin pigmentation that should not be confused with signal. (**o**–**v**) Whole-mount tail epidermal sheets, prepared from P22-P55 *hK6a*-LacZ transgenic mice, were dual-immunostained using antibodies directed at (**o**–**u**) LacZ and either (**p**, **t**) K6, (**r**) K17, or (**v**) the IRS marker trichohyalin, before analysis by confocal microscopy. Micrographs are labeled as above, and arrows denote labeling. The anti-mouse secondary antibody used yields nonspecific staining on sebaceous glands (SG). Bar = 50 μm.

We performed dual indirect immunofluorescence on whole-mount tail skin preparations to compare the distribution of LacZ antigens to that of K6 and its partner K17. Stained preparations were visualized by confocal microscopy. In anagen follicles, nuclear LacZ antigens form a thin layer that coincides with cytoplasmic K6 antigens (Figure 2o and p, anagen V). In catagen follicles, a single row of LacZ-positive nuclei corresponds to the innermost portion of K17-positive (Figure 2q and r; catagen I) and K6-positive tissue (Figure 2s and t; catagen VIII). In telogen follicles, LacZ staining occurs

mostly as a concentric ring below the sebaceous glands (Figures 1 and 2), whereas K17 antigens are present in the entire club sheath (Bernot *et al.*, 2002) (data not shown). Dual staining for trichohyalin and LacZ antigens revealed that the LacZ signal is immediately outside of the IRS (Figure 2u and v), indicating that LacZ protein is restricted to the CI.

Proliferation status of *mK6a*-expressing cells in cycling hair follicles

We next ascertained the proliferation status of *hK6a*-LacZ expressing cells, identified via antibody staining, through BrdU immunolocalization studies. BrdU incorporation regimens were varied so as to localize either slow cycling or rapidly cycling keratinocytes. BrdU treatment was first conducted to assess whether hK6a-LacZ expressing cells are slow cycling (Cotsarelis *et al.*, 1990; Bickenbach and Chism, 1998; Braun *et al.*, 2003). We found that BrdU-positive nuclei are distinct from, and located external to, LacZ-positive ones (Figure 3b–c) in the postnatal telogen follicles (P53). Lack of colocalization between CD34, a marker enriched in bulge epithelial stem cells in the mouse (Trempus et al., 2003; Morris *et al.*, 2004; Tumbar *et al.*, 2004), and K6 antigens, which are present in the hair proximal cell layers (Blanpain *et al.*, 2004) provide further support for this interpretation (Figure 3d–i). We also treated *hK6a*-LacZ mice of various age with BrdU 2 hours before skin tissue analysis to determine whether the cells turning on *hK6a*-LacZ expression during anagen are actively proliferating. Of the large group of cells that are BrdU-positive as anagen progresses, only a small faction are LacZ-expressing as well (Figure 3j–l).

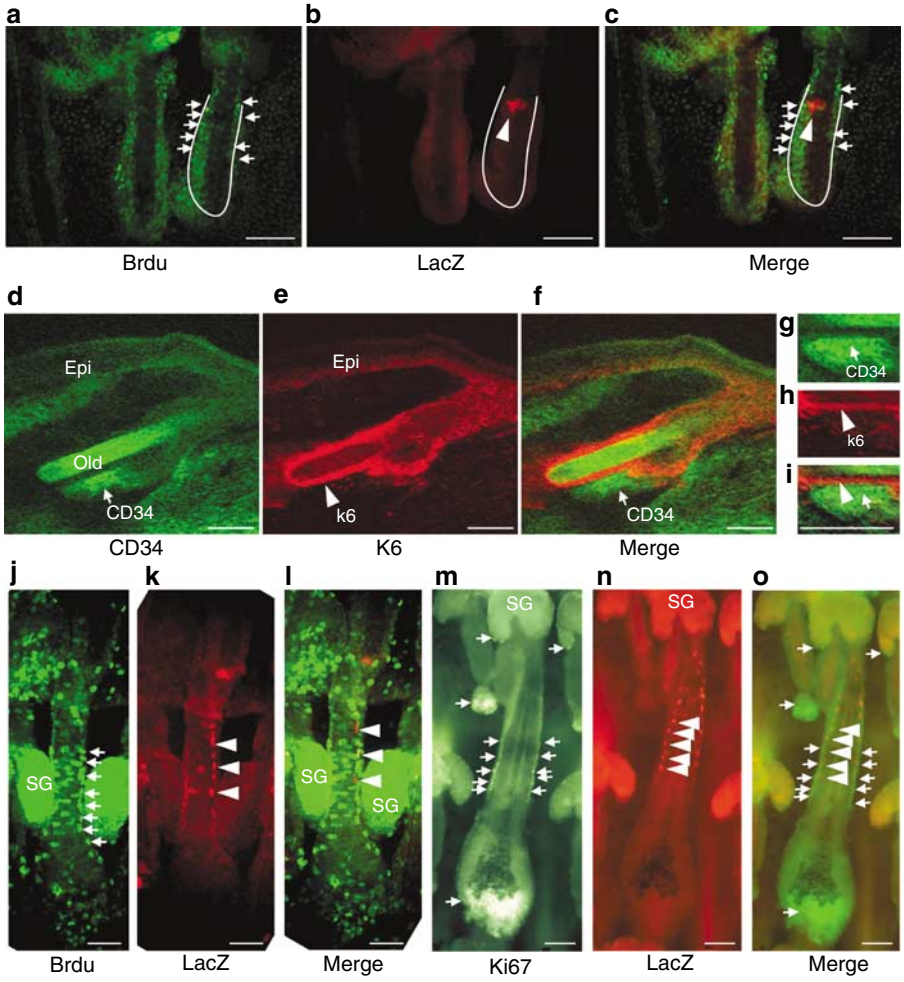

Figure 3. Proliferating status of *hK6a*-LacZ-expressing cells during postnatal hair follicle cycling. (**a–c**) *hK6a*-LacZ mice were treated with BrdU for the detection of either slow-cycling cells or (**j–l**) actively proliferating cells. At the designated times (see Materials and Methods), mice were killed, and tail skin samples were processed for dual-immunostaining using antibodies directed against the antigens identified below each micrograph. (**a–c**) Dual stain for BrdU, identifying slow-cycling cells (arrows), and LacZ (arrowhead). The two signals do not coincide. (**d–f**, **g–i**) Dual stain for CD34 (arrows), a marker enriched in epithelial stem cells of the bulge, and K6 (arrowhead). Again, the two signals do not coincide. The secondary antibody used to detect anti-CD34 reacts nonspecifically with the hair shaft (see ''old'' in **d**). In **g–i**, the bulge region from a follicle oriented sideways is highlighted. (**j–l**) Dual stain for BrdU, identifying S-phase (actively proliferating) cells (see arrows in **j**), and LacZ (arrowheads in **k**), imaged using confocal microscopy. The two signals coincide very rarely. (**j–l**) Dual stain for Ki67, identifying cycling cells (arrows in **j**), and LacZ (arrowheads in **k**), imaged using a standard epifluorescence microscope. Again, the two signals do not coincide. (**m–o**) Dual stain for Ki67, identifying cycling cells (arrows in **m**), and LacZ (arrowheads in **n**), imaged using a standard epifluorescence microscope. Bar = 50 μm.

Conversely, few LacZ-expressing cells are BrdU-positive as well (see Figure 3j–l for an example). We extended this analysis by performing dual immunostaining for LacZ and Ki67, a marker present in all phases of the cell cycle except G0. Ki67 immunoreactivity is strong in the outmost cell layer of sebaceous gland, secondary hair germ cells, hair matrix cells, and ORS of anagen follicles (Figure 3m and data not shown). LacZ immunoreactivity signal occurred proximal to, but did not coincide with, Ki67 (Figure 3n and o; anagen IIIc). These results suggest that *K6a* expression is turned on as, or after, the relevant subset of progenitor keratinocytes commit to differentiation following anagen re-entry (see Discussion).

mK75 and trichohyalin show a regulation that is temporally and spatially distinct from *mK6a*

K75 is a relatively new type II keratin gene (Winter *et al.*, 1998), and is expressed in the Cl and medulla in human and mouse hair follicles (Wojcik *et al.*, 2001; Wang *et al.*, 2003). Its regulation during hair cycling has not been characterized, though it is known that the *mK75* mRNA does not occur in telogen-stage mouse hair follicles (Wang *et al.*, 2003). To address this gap, *in situ* hybridization for *mK75* mRNA was carried out on whole-mount tail skin preparation exactly as performed for *mK6a* (Figure 1). No signal for the *mK75* mRNA could be detected in telogen-stage tail skin follicles (Figure 4a) or during anagen I/II (Figure 4b). A strong, triangle-shaped hybridization signal appears in the follicle center, right above the newly formed bulb region, at anagen IIIa (Figure 4c). The hybridization signal progressively expands downward (Figure 4d and e), and especially upward, during anagen IIIb (Figure 4f), anagen IIIc (Figure 4g), anagen IV (Figure 4h), and anagen V and VI (Figure 4i–j). During catagen, the signal for K75 mRNA adopts a characteristic cup shape at the base of the involuting hair (Figure 4k–m). The sense probe yielded background staining (Figure 4n), establishing signal specificity. Of note, strong hybridization for the *mK75* mRNA was detected in the medulla of many follicles (e.g., see asterisks in Figure 4i and k), suggesting that probe penetration is not a limiting factor in these preparations.

The spatiotemporal pattern exhibited by the *mK75* mRNA during hair cycling in tail skin, with appearance in the core region of the bulb at anagen IIIa and gradual spreading towards the bulge area, is reminiscent of what has been reported for IRS markers in pelage skin (Aoki *et al.*, 2001; Porter *et al.*, 2001; Langbein *et al.*, 2002, 2003). To confirm that this also applies to tail skin follicles visualized in whole-mount preparations, we immunolocalized trichohyalin, an established marker of the IRS and medulla (O'Guin *et al.*, 1992). As expected, trichohyalin cannot be detected before anagen IIIa (e.g., Figure 4o and p), at which time it adopts the characteristic triangular-shaped signal above the hair bulb (Figure 4, q, r, s, and t). At later stages of anagen (IIIa/b: Figure 4u; IIIb: Figure 4v; IIIc: Figure 4w) and in all other stages of anagen examined, the pattern seen for trichohyalin was similar to that of *mK75*. Altogether these observations establish for the first time that a Cl marker, *K75*, is temporally and spatially regulated in a pattern that is highly analogous to markers of the IRS and hair shaft.

Specialized Huxley cells (Flügelzellen) occurs in mouse hair follicles

To better appreciate the intimate features of Cl in anagen hair follicles, we examined pelage hair follicles of P5 wild-type mice by transmission electron microscopy. At that stage, maturing follicles are at stage 7/8 (Paus *et al.*, 1999), which is similar to anagen III/IV follicles during postnatal hair cycling (Muller-Rover *et al.*, 2001). Hair follicles sectioned longitudinally along their equatorial plane were selected for study. Figure 5a and b, shows hair follicle tissue at low magnification in the suprabulbar region and at a higher level, below the isthmus, respectively, corresponding to intermediate and advanced differentiation stages. In both instances, the He is terminally differentiated, the cuticles of the hair shaft (Cu_h) and IRS (Cu_i) are interlocked owing to their inverted, complementary topology (shown by arrows), and the Cl appears as a monolayer of thin, elongated cells tightly apposed against the He. When the more advanced stage of differentiation corresponding to Figure 5b is viewed at a higher magnification, numerous desmosomes connecting the He and Cls (see arrowheads in Figure 5c) can be seen, as well as large bundles of keratin filaments (K) in the cytoplasm of Cl cells, polarized on the He side (Figure 5b and d). By comparison, the interface between the Cl and the ORS contains markedly fewer adhesion complexes and keratin filaments (Figure 5c and d). The higher density of keratin filaments occurring at the advanced stage of Cl differentiation corresponds to the zone of maximal overlap between the domains of *mK6a* and *mK75* expression (Figures 1 and 4). These studies also revealed the presence of gaps between differentiated cells of the He, allowing for Huxley layer cells to reach out for, and tightly adhere to, Cl cells (see arrowheads in Figure 5e). Such structures, termed *Flügelzellen* (Clemmensen *et al.*, 1991; Langbein *et al.*, 2002; Alibardi, 2004), have not been described in mouse before. These ultrastructural observations indicate the Cl forms a tight connection with the IRS (specifically the He and Huxley layers), which is itself tightly integrated with the hair shaft, during hair growth.

mK6a expression in human hair follicles and in the mouse nail unit

To further substantiate that *K6a* and *K75* are both expressed in the Cl, we turned to human skin tissue as a guinea pig antiserum that is monospecific for hK75 protein is available (Winter *et al.*, 1998; Wang *et al.*, 2003). We find that hK6 and hK75 antigens colocalize in a thin cell layer of anagen-stage hair follicles on human scalp sections (5f–h). This layer is located immediately inside of the ORS, visualized through K14 staining (data not shown). Given that the *hK6b* mRNA occurs at low levels in normal human skin (Takahashi *et al.*, 1995), the signal detected using our rabbit anti-K6 antiserum (McGowan and Coulombe, 1998; Wang *et al.*, 2003) mostly reflects hK6a protein. This confirms that both K6a and K75 occur in the Cl of human hair follicles.

The nail features a region, the interface between the growing nail plate and stationary nail bed, that is functionally analogous to the Cl/ORS interface in hair

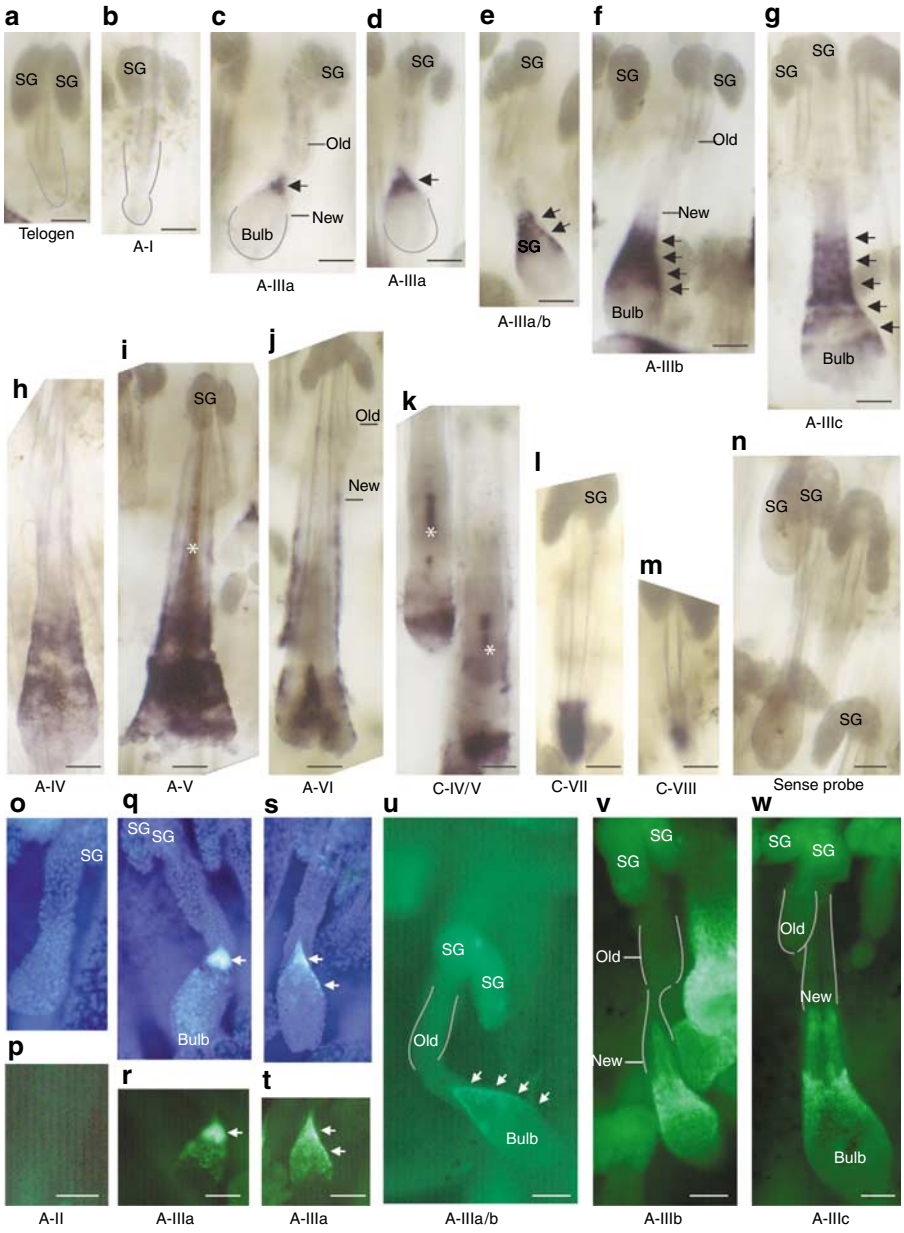

Figure 4. Regulation of *mK75*, a Cl marker, during postnatal hair follicle cycling in mouse. (**a**–**n**) Whole-mount tail epidermal sheets, prepared from P22-P55 wild-type mice, were hybridized with (**a**–**m**) antisense and (**n**) sense probes specific for the *mK75* mRNA. Hair cycle stage is indicated below each micrograph. (**a**–**d**) A line depicts the outer limit of relevant areas of the follicle. No hybridization was detected during (**a**) telogen or (**b**) anagen I. A signal first appeared at anagen IIIa (see arrows in **c**, **d**), in a region located right above the bulb. Subsequently, between anagen IIIb and anagen VI, the hybridization signal intensified and progressively extended upward, towards the bulge region (see **e**–**j**). (**k**–**m**) During catagen, the signal becomes restricted to the narrowing base of the involuting follicles. A strong signal for the *mK75* mRNA can often be seen in the medulla (asterisks in **i**, **k**), as expected (Wang *et al.*, 2003), suggesting the probe penetration is not a limiting factor. (**n**) Use of the sense probe yielded only background staining. (**o**–**w**) Whole-mount tail epidermal sheets, prepared from P22-P55 wild-type mice, were dual-immunostained using the vital dye Hoechst (to visualize nuclei) and an antibody directed at trichohyalin, an IRS marker, before analysis via standard epifluorescence microscopy. The results obtained are nearly identical as for the *mK75* mRNA. See text for more details. SG, sebaceous gland; bulb, hair bulb. Bar = 50 μm.

follicles. Intriguingly, this region is also enriched for K6 antigens along with expression of the *hK6a-LacZ* transgene (Figure 5i and j). These results suggest that *K6a* (and K75; Wang *et al.*, 2003) is expressed in functionally similar regions in the growing hair and nail plate.

DISCUSSION

The mK6a mRNA seemingly does not occur in slow-cycling epithelial cells of the hair bulge

Other researchers reported that the *mK6a* mRNA (Morris *et al.*, 2004; Tumbar *et al.*, 2004), or K6 protein (Trempus

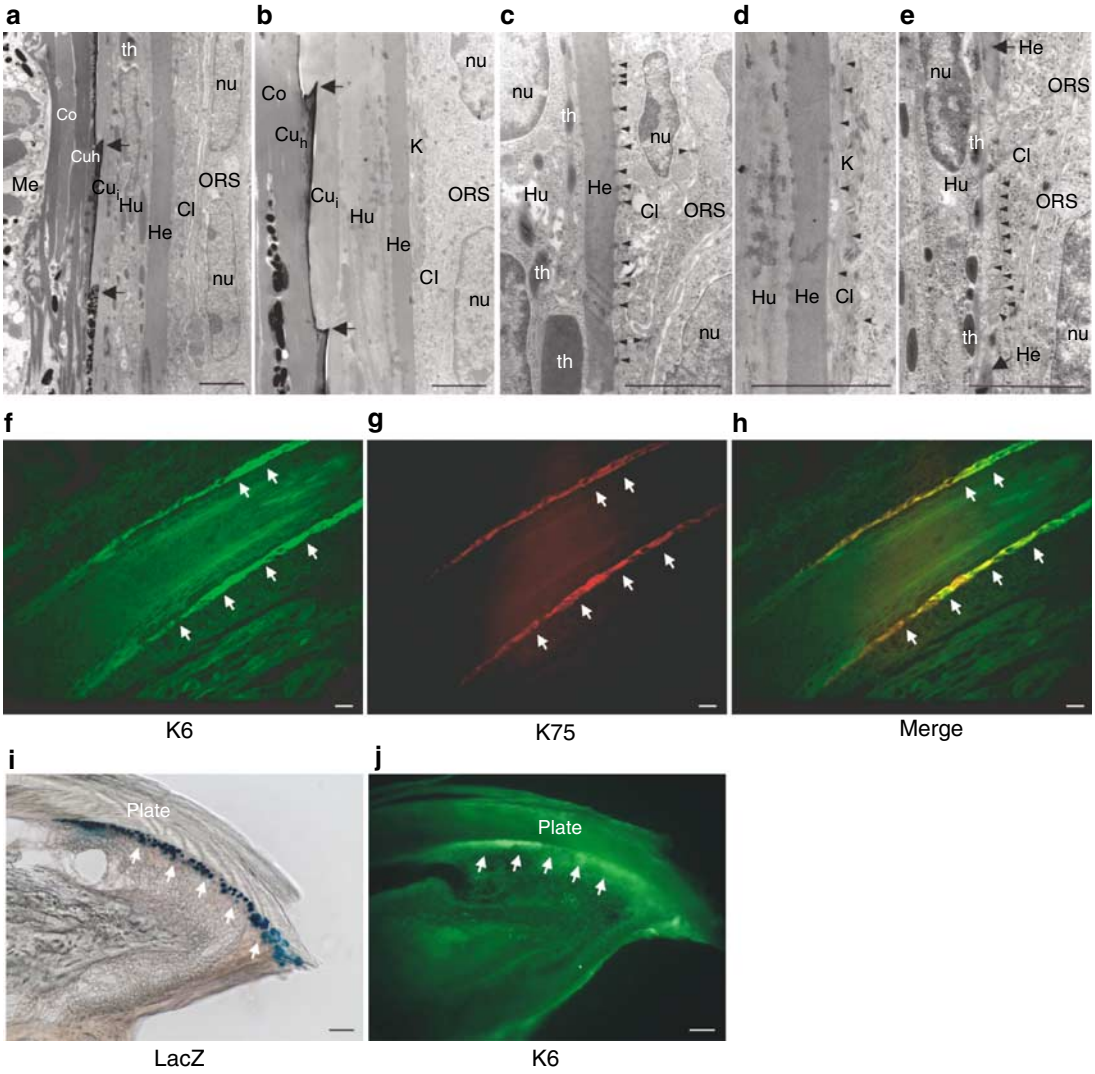

Figure 5. Additional observations on the Cl, and parallel with nail tissue. (**a**–**e**) Transmission electron microscopy of longitudinally sectioned anagen-stage hair follicles in P5 wild-type mice. In all cases, that hair is growing in the upper direction. (**a** and **b**) show low magnification surveys extending from the hair shaft to the ORS, whereas (**c**–**e**) are higher magnification views detailing the interface between IRS and Cl. (**c**) The interface between the Henle (He) and Cl features a high density of desmosomes, in contrast to the contralateral side, where a fine gap separates the Cl cell membrane form that of proximal ORS epithelial cells. (**d**) Arrowheads point to large keratin filament bundles (K) in the cytoplasm of Cl cells, proximal to the He. (**e**) Direct contact, and formation of a tight adhesive interface, between Huxley layer cells and Cl cells. Such contacts, termed flügelzellen, are made possible because of gaps between differentiated He cells. Cl, companion layer, Cu_h, cuticle of the hair shaft; Cu_i, cuticle of the IRS; Co, cortex of the hair shaft; He, Henle layer; Hu, Huxley layer; K, keratin filament bundles; Me, medulla of the hair shaft; nu, nucleus; ORS, outer root sheath; th, trichohyalin. Bar = 2 μm. (**f**–**h**) Dual immunofluorescence showing the colocalization of hK6 and hK75 in anagen-stage hair follicles in sections prepared from human scalp. Bar = 50 μm. (**i** and **j**) Longitudinal cross-sections of nail tissue prepared from *hK6a*-LacZ transgenic mice, and processed for (**i**) X-gal staining and (**j**) K6 immunostaining in hK6*a*-lacZ mice are expressed in the nail bed in the front region of nail tissue. In both instances, there is a strong signal in the nail bed epithelium (arrows). Bar = 50 μm.

et al., 2003), is enriched in sorted epithelial stem cells originating specifically from the bulge region of hair follicles (for different results, however, see Blanpain *et al.*, 2004; Ohyama *et al.*, 2006). K6 is also considered as a progenitor cell marker in a different epithelial setting, that is, mammary glands (Smith and Chepko, 2001; Li and Rosen, 2005). Our *mK6a* mRNA localization and BrdU incorporation studies yielded a different outcome, that is, that *mK6a* is not expressed in the slow-cycling epithelial cells of the hair bulge. In support of this interpretation, Cre recombinase-mediated activation of a highly sensitive reporter transgene remains restricted to the Cl in mouse pelage skin when placed under the control of the *mK6a* gene promoter (Smyth *et al.*, 2004). Were the *mK6a* gene transcribed in pluripotent hair progenitor cells, the domain of Cre-activated reporter expression clearly would exceed the boundaries of the Cl in these mice. This said, *mK6a* expression occurs proximal to the bulge, and persists in the innermost layer of the club hair sheath, making such determinations technically challenging. Moreover, the *mK6a* gene may be subjected to complex transcriptional and post-transcriptional regulatory mechanisms (e.g., Lu *et al.*, 2005) that may not be fully reproduced in

the *hK6a-LacZ* (this study) and *mK6a*-Cre transgenic mice (Smyth *et al.*, 2004). Ultimately, more information on the properties and roles of the innermost epithelial layer in the club hair sheath (e.g., Blanpain *et al.*, 2004; Ito *et al.*, 2004) should help revolve the issue of whether *mK6a* is expressed in any progenitor (stem) cell population.

The Cl forms alongside the IRS layers during anagen re-initiation in mouse, and is functionally integrated with the IRS and hair shaft during hair growth

Our study of *mK6a* and *mK75* mRNA localization during postnatal hair follicle cycling, using whole-mount assays in mouse tail skin epithelia (Braun *et al.*, 2003), yielded exciting new insight into the morphogenesis of the Cl and the regulation of gene expression as telogen hair follicles re-enter anagen. As is already established for markers of both the IRS (e.g., trichohyalin; this study) and hair shaft (see Muller-Rover *et al.*, 2001), the *mK75* mRNA can be first detected in the upper portion of the newly formed hair bulb, in a characteristic cone-shaped pattern, at anagen IIIa. Thereafter, *mK75* expression progressively extends towards the isthmus, in a ''bulb-to-bulge'' direction, as follicles progress further into anagen. This pattern is similar to trichohyalin, an established IRS marker. In anagen stage follicles, K75 occurs in the Cl, a single row of cells located between the IRS and ORS compartments, and in the medulla of the hair shaft (Winter *et al.*, 1998; Wang *et al.*, 2003). Based on evidence introduced here and elsewhere (Ito, 1986; Winter *et al.*, 1998; Wang *et al.*, 2003), the Cl originates from the upper matrix of the hair bulb concomitant with the IRS layers.

Ultrastructural findings also provide strong support for the notion that the Cl, IRS, and hair shaft are integrated into one functional unit during hair growth. Relative to the interface with He, which features extensive tight junctional and desmosomal cell–cell contacts, many fewer adhesions occur between the Cl and ORS layer (Figure 5a and c; Ito, 1986, 1988). In addition to this intimate connection between the Cl and He, specialized Huxley cells extend cytoplasmic bridges, through rather wide ''gaps'' occurring between differentiated He cells, which directly contact the Cl. These remarkable structures, termed *Flügelzellen*, have been previously described in human and marsupial hair follicles (Clemmensen *et al.*, 1991; Langbein *et al.*, 2002; Alibardi, 2004), though their functional significance is unknown. Here, we establish that they also exist in mouse (Figure 5e). In regards to the interface between the IRS and hair shaft, it has again long been known that their cuticles are tightly interlocked owing to their complementary topology (Figure 5a and b; also, see Hashimoto and Shibazaki, 1976; Abell, 1994, for similar data from human hair follicles). The resulting Cl/IRS/hair shaft unit is able to ''glide'' along the inner aspect of the ORS, a compartment with distinct cellular origin and overall properties, during anagen. The tight interlinking of these three compartments (hair shaft, IRS, and Cl) likely provides a tubular frame that guides the growing hair during its ascension towards the surface. When this unit reaches the isthmus, the hair shaft breaks free from surrounding sheaths, which are sloughed off in the hair canal (Ito, 1989; Winter *et al.*, 1998; Langbein *et al.*, 2002; Langbein and Schweizer, 2005). This model calls for an exquisite degree of coordination in the rate of cell production and differentiation in the seven epithelial lineages originating from epithelial precursors housed in the hair matrix.

A conceptually similar ''tissue engineering'' problem occurs as the growing nail plate is gliding along the nail bed epithelium (Wong *et al.*, 2005). Of interest, a similar complement of keratin proteins occurs at this interface as well (De Berker *et al.*, 2000; McGowan and Coulombe, 2000). In *hK6a-LacZ* mice, for instance, reporter activity can be readily detected in the nail bed, which also expresses K6 antigens.

Together with the literature discussed above, the new findings reported in the study raise the distinct possibility that the Cl is an integral part of the IRS compartment in hair follicles. By virtue of the location of its progenitors in the hair matrix, the timing and location of its formation soon after anagen re-entry (as seen, specifically, through *mK75* expression), and its ultrastructural integration with the IRS layers and hair shaft, the Cl certainly is more akin to the IRS than the ORS compartment. If so, the master regulators of the IRS lineage should initiate Cl morphogenesis as well. K6 gene expression is ''retained'' in the grossly abnormal hair follicles of GATA-3 null mice, which show specific defects in the IRS lineage (Kaufman *et al.*, 2003), but this phenomenon likely reflects the exquisite sensitivity of the K6/K16 pair to aberrant differentiation in the ORS compartment.

The significance of differential keratin expression in the Cl is unclear

Although both the *mK75* and *mK6a* genes are expressed in the Cl of anagen-stage follicles, we show here that the latter shows a strikingly distinct regulation during postnatal hair cycling. Thus, the *mK6a* mRNA is first detected in cells located adjacent to the club hair epithelium, starting at anagen IIIb. Thereafter the domain of *mK6a* mRNA expression spreads towards the newly generated bulb as follicles progress further into anagen. These findings are corroborated by studies of mice in which the expression of a LacZ reporter is placed under the control of the human orthologous gene promoter (*hK6a*) (Takahashi and Coulombe, 1996, 1997). As reported here, transgenic *hK6a* expression rarely occurs in proliferating cell in postnatal hair follicles, and could not be deteted in slow-cycling cells. In regenerating hair follicles, therefore, *mK6a* regulation differs from that of *mK75* and markers of the IRS/hair shaft in several respects, including the timing and location of its appearance, and its subsequent progression in time.

Ultrastructurally, prominent keratin filament bundles can be seen in Cl cells, specifically on the He side (e.g., Figure 5b and d), starting in the mid-section of the hair follicle. These bundles have been described before (Ito, 1986, 1988). Together with the high density of cell–cell adhesions between the companion and He (and possibly, the enigmatic *Flügelzellen*), the presence of such bundles likely fosters locally high mechanical strength in Cl cells, on the IRS side. By comparison, the lower density of keratin filament bundles

occurring on the other side of the cell, facing the ORS, likely fosters a less adhesive interface, and presumably, allow for gliding while avoiding intracellular rupture. Whether K6a and K75 proteins are partially segregated, or completely integrated (and intermixed) within the asymmetrically organized keratin network of the Cl, is unknown at this time. Besides, the distinct spatiotemporal regulation exhibited by *K6a* and *K75* mRNA following anagen re-entry could serve a purpose other than, or in addition to, modulating the mechanical support function of keratin filaments (Coulombe and Wong, 2004; Kim *et al.*, 2006). These issues certainly are worth pursuing in follow-up studies.

Implications for the pathophysiology of Cl and nail disorders

Genetic evidence in both human (Winter *et al.*, 2004) and mouse (Wojcik *et al.*, 1999) establishes that altering keratin filaments in the Cl significantly compromises the shape and path of the hair shaft as it grows towards the tissue surface. Pseudofolliculitis barbae is a common Cl disorder with a higher prevalence in African American males and other people with curly hair. The problem arises as a result of shaving, causing highly curved hairs to grow back into the skin and trigger a local inflammation and foreign body reaction. A particular missense mutation, Ala_{12}->Thr, in *K75* has been identified as a risk factor in this disorder (Winter *et al.*, 2004). Mutations in *K6a* and *K6b* genes cause the nail bed disorder pachyonychia congenita (Bowden *et al.*, 1995; Smith *et al.*, 1998, 1999; Lin *et al.*, 1999; Terrinoni *et al.*, 2001; Ward *et al.*, 2003). In addition to the hallmark nail dystrophy, pachyonychia congenita patients often exhibit hair anomalies such as *pili torti*, in which the hair is twisted and mechanically fragile (Clementi *et al.*, 1986; Feinstein *et al.*, 1988; Dahl *et al.*, 1995; McLean *et al.*, 1995; Templeton and Wiegand, 1997). Based on genetic evidence gathered from mouse studies, it is highly likely that the impact of mutations in either *K6a* or *K6b* is mitigated by their markedly redundancy function (Wong *et al.*, 2000; Wojcik *et al.*, 2001). Loss of both *mK6a* and *mK6b* causes marked epithelial fragility in the oral mucosa (Wong *et al.*, 2000; Wojcik *et al.*, 2001) and at the edge of skin wounds (Wong and Coulombe, 2003), reflecting a mechanical support role in these settings. Likely owing to *K75* (Wojcik *et al.*, 2001), however, it has been difficult to ascertain the role of *mK6a* and *mK6b* in hair follicles, and in particular, in the Cl. The use of Cl-specific gene rearrangement (e.g., Smyth *et al.*, 2004) to conditionally inactivate the *K6a*, *K6b*, and *K75* loci, and replace them with one type II keratin gene at a time, may help resolve the contribution of individual keratins to the properties of the Cl *in vivo*.

MATERIALS AND METHODS

Keratin nomenclature

The novel keratin nomenclature devised by Schweizer *et al.* (2006) is in use in this article. The *mK6a* and *mK6b* gene were formally designated as *mK6α* and *mK6β*, respectively (Takahashi *et al.*, 1998; Wong *et al.*, 2000), whereas the *mK75* gene was formerly known as *mK6hf* (Winter *et al.*, 1998; Wojcik *et al.*, 2001; Wang *et al.*, 2003).

Animal model, whole-mount epidermal sheets preparation, and hair cycle analysis

All protocols for mouse experimentation were reviewed and approved by the Johns Hopkins University Animal Care Use Committee. Two previously described lines of *hK6a-LacZ* mice (23-3 m, 23-1p), harboring a transgene featuring 5.2 kb of 5′upstream sequence from the *hK6a* gene, were used (Takahashi and Coulombe, 1997). Whole-mount epidermal sheets were prepared from mouse tail skin as described (Braun *et al.*, 2003). Briefly, tail skin was slit along its main axis, peeled from the bone, and cut into square-shaped pieces. After incubation in 5 mM EDTA in phosphate-saline buffer (PBS) for 4–6 hours at 37°C, epidermal sheets were gently peeled away from the tissue, prepared and used for various analyses. Because of the focus on hair cycling, all epidermal sheets were obtained from the same region on the dorsal side of the tail. Hair cycle stage was determined based on mouse age along with the morphological criteria defined by Müller-Röver *et al.* (2001). Hair follicle cycling proceeds identically in mouse tail and pelage skin (Gu and Coulombe, unpublished data).

Antibodies, probes, and other reagents

We used a rabbit polyclonal antiserum raised against a K6 C-terminal peptide epitope (''K6gen'', McGowan and Coulombe, 1998) that reacts equally well with the classic K6 isoform a and b, but not with K75 or K5 (Wang *et al.*, 2003). Other antibodies used included rabbit polyclonal antisera directed against K14 (AF64, Covance Inc., Princeton, NJ), K17 (McGowan and Coulombe, 1998), Ki67 (VP-K451, Vector lab, UK) and LacZ/*β*-galactosidase (ab616, Abcam Ctd); a guinea-pig polyclonal antiserum directed against K75 (Winter *et al.*, 1998); mouse monoclonal antibodies directed against LacZ/*β*-galactosidase Ab (40-1a, Developmental study hybridoma bank, University of Iowa), trichohyalin (AE15, O'Guin *et al.*, 1992) and BrdU (B9285, Sigma Chem Co., St Louis, MO); and a rat monoclonal antibody against CD34 (clone RAM34, BD Bioscience, Rockville, MD). Rhodamine- or FITC-conjugated goat anti-mouse, anti-rabbit, anti-guinea, or anti-rat secondary antibodies were obtained from Kirkegaard and Perry Labs (Gaithersburg, MD). *In situ* hybridization for the *mK6a* and *mK75* mRNA was performed using antisense and sense (control) probes as described (Takahashi *et al.*, 1998; Wang *et al.*, 2003).

Routine histological analyses

For indirect immunofluorescence, whole-mount epidermal sheets were fixed in 4% paraformaldehyde at room temperature for 20 minutes, rinsed in PBS (2 × 10 minutes), blocked and permeabilized by incubation in phosphate–borate buffer (0.5% skim milk powder, 0.25% fish skin gelatin, 0.5% Triton X-100 in 0.9% NaCl/20 mM *N*-2-hydroxyethylpiperazine-*N*′-2-ethanesulphonic acid pH 7.2) for 30 minutes (Braun *et al.*, 2003). The sheets were then incubated with properly diluted primary antibodies for ~36 hours with gently agitation, washed in PBS containing 0.2% Tween 20 (4 × 1 hour), and then incubated in FITC-or Rhodamine-conjugated secondary antibodies overnight. Epidermal sheets were washed again in PBS containing 0.2% Tween 20, rinsed in distilled water and mounted in Movoil mounting media. Preparations were visualized using either a Zeiss Axioplan-2 microscope equipped for epifluorescence or a PerkinElmer UltraView confocal microscope.

For β-galactosidase histochemistry, samples were rinsed once in 2 mM $MgCl_2$/PBS and fixed in 0.5% glutaraldehyde/PBS for 15 minutes at room temperature. They were then washed in 2 mM $MgCl_2$/PBS (2 × 5 minutes) and incubated in freshly prepared 1 mg/ml X-gal (5-bromo-4-chloro-3-indolyl-beta-D-galactopyranoside, G-5001-0101, ISC, BioExpress) in X-gal solution containing 100 mM Na_2HPO_4/NaH_2PO_4 (pH 7.3), 2 mM $MgCl_2$, 3 mM $K_3Fe(CN)_6$, 3 mM $K_4Fe(CN)_6$, 0.01% Na-deoxycholate, 0.02% NP-40 for 1 hour at 37°C. After incubation, the samples were washed once in 2 mM $MgCl_2$/PBS and mounted with crystal mount media (Biomeda, Foster city, CA). Samples were then analyzed and images captured using a light microscope.

Mouse tissue (nail and tail) were obtained from adult mice and embedded in OCT (Sakura Finetec, Torrance, CA), 10–20 μm frozen sections were obtained before fixation.

Transmission electron microscopy

Pelage skin from 5-day-old wild-type C57Bl/6 mice was fixed in 0.1 M sodium cacodylate buffer (pH 7.2) containing 2% glutaraldehyde/1% paraformaldehyde, post-fixed in 1% osmium tetroxide/0.1 M phosphate buffer, and embedded in LX112 epoxy resin (Ladd Research Industries Inc., Burlington, VT) as described elsewhere (Paladini and Coulombe, 1999; McGowan *et al.*, 2002). Thin (50–70 nm) sections were counterstained with uranyl acetate and lead citrate, and visualized using a Philips CM120 electron microscope. Longitudinally sectioned hair follicles containing the entire hair axis were selected for study.

BrdU incorporation and localization

For short-term labeling, mice were intraperitoneally injected with BrdU (100 mg/kg) 2 hours before killing. For long-term labeling, P10 mice were intraperitoneally injected with BrdU (50 mg/kg body weight) every 12 hours for a total of four injections and killed at P52–P55 for analysis. For BrdU localization, 4% paraformaldehyde pre-fixed whole-mount epidermal sheets were denatured in 2 M HCL at 37°C for 30 minutes, neutralized twice in 0.1 M borate buffer, pH 8.5 for 5 minutes, and washed twice in PBS for 5 minutes. Samples were then treated with 0.2% Triton X-100 for 30 minutes, washed three times in PBS, and immunostained as described above.

In situ hybridization on whole-mount epidermal sheets

All reagents and containers used were 0.1% diethylpyrocarbonate (DEPC)-treated. Whole-mount epidermal sheets were fixed in 4% paraformaldehyde at 4°C overnight then dehydrated through graded methanol (25, 50, 75, 100%) in PBS and stored at −20°C until use. Subsequent steps were carried out in sterile 12-well plates over 2 days at room temperature unless mentioned otherwise.

Pre-fixed tail epidermal sheets, warmed to room temperature, were re-hydrated through 75, 50, 25% methanol in PBS (5 minutes each) and washed in PBST (0.2% Tween20 in PBS) (3 × 5 minutes). After PBS rinses, samples were then further fixed in 4% paraformaldehyde (10 minutes) followed by proteinase K (20 μg/ml in 200 mM $CaCl_2$/PBS; pre-warmed at 37°C) digestion for 15 minutes. Samples were washed in PBST (3 × 10 minutes), post-fixed in 4% paraformaldehyde in PBS for 20 minutes, washed again in PBST (2 × 10 minutes), briefly incubated in 0.1 M TEA buffer (1 minute) and then in 0.25% acetic anhydride in 0.1 M TEA buffer (10 minutes). After additional washes in PBST (2 × 10 minutes), samples were permeabilized in 0.1% Triton X-100 in PBS for 30 minutes. After three washes in PBST (10 minutes each), samples were incubated for 1 hour at 65°C in pre-warmed hybridization solution (10% Dextran sulfate, 5 × Denhardt's reagent, 1 M NaCl, 50% formamide, 500 μg/ml tRNA). 1 μg/ml probe was added to pre-warmed hybridization solution, heated at 85°C for 3 minutes, and then immediately mixed with the sample for an overnight incubation at 65°C. The next day, the hybridization solution was removed and samples rinsed in freshly prepared washing solution (50% formamide, 0.5 × standard sodium citrate, 0.1% Tween 20) at 65°C, and incubated in this washing solution for 2 hours at 65°C. Following a wash in 0.2 × standard sodium citrate at 72°C for 15 minutes, epidermal sheets were brought back to room temperature in 0.2 × standard sodium citrate, transferred to blocking solution (3% normal goat serum, 3% fetal bovine serum in PBS) for 30 minutes, followed by an incubation in alkaline phosphatase (AP)-conjugated sheep anti-DIG-fab fragments (diluted 1:1,000 in blocking solution containing 0.3% Tween 20) for 4 hours to overnight at 4°C in the dark. Epidermal sheets were then washed with PBS (5 × 15 minutes), rinsed in AP buffer (100 mM Tris-HCl, pH 9.5, 100 mM NaCl, 50 mM $MgCl_2$) for 10 minutes, and incubated in freshly prepared developer solution (4 μl/ml nitroblue tetrazolium, 3 μl/ml 5-bromo-4-chloro-8-indolilphosphate (BCIP), 0.2 mg/ml levamizole in AP buffer) for 12–16 hours. This reaction is stopped by washing the samples with PBS for 10 minutes, and hybridized epidermal sheets are mounted in crystal/mount media in preparation for microscopy.

CONFLICT OF INTEREST

The authors state no conflict of interest.

ACKNOWLEDGMENTS

We thank Dr Henry Sun, Dr Michael O'Guin, and Dr Lutz Langbein for their gift of antibodies, Dr Carol Trempus, Dr Sarah Millar, and Dr George Cotsarelis for comments, and members of the Coulombe laboratory for support. These studies were supported by NIH Grant AR42047.

REFERENCES

Abell E (1994) Embryology and anatomy of the hair follicle. In: *Disorders of Hair Growth* (Olsen EA, ed), New York: McGraw-Hill Inc., 1–19

Alibardi L (2004) Fine structure of marsupial hairs, with emphasis on trichohyalin and the structure of the inner root sheath. *J Morphol* 261:390–402

Alonso L, Fuchs E (2003) Stem cells of the skin epithelium. *Proc Natl Acad Sci USA* 100:11830–5

Aoki N, Sawada S, Rogers MA, Schweizer J, Shimomura Y, Tsujimoto T *et al.* (2001) A novel type II cytokeratin, mK6irs, is expressed in the Huxley and Henle layers of the mouse inner root sheath. *J Invest Dermatol* 116:359–65

Bernot K, McGowan K, Coulombe PA (2002) Keratin 16 expression defines a subset of epithelial cells during skin morphogenesis and the hair cycle. *J Invest Dermatol* 119:1137–49

Bickenbach JR, Chism E (1998) Selection and extended growth of murine epidermal stem cells in culture. *Exp Cell Res* 244:184–95

Blanpain C, Lowry WE, Geoghegan A, Polak L, Fuchs E (2004) Self-renewal, multipotency, and the existence of two cell populations within an epithelial stem cell niche. *Cell* 118:635–48

Bowden PE, Haley JL, Kansky A, Rothnagel JA, Jones DO, Turner RJ (1995) Mutation of a type II keratin gene (K6a) in pachyonychia congenita. *Nat Genet* 10:363–5

Braun KM, Niemann C, Jensen UB, Sundberg JP, Silva-Vargas V, Watt FM (2003) Manipulation of stem cell proliferation and lineage commitment:

visualisation of label-retaining cells in whole mounts of mouse epidermis. *Development* 130:5241–55

Clementi M, Cardin de Stefani E, Dei Rossi C, Avventi V, Tenconi R (1986) Pachyonychia Congenita Jackson Lawler type: a distinct malformation syndrome. *Br J Dermatol* 114:367–70

Clemmensen OJ, Hainau B, Hansted B (1991) The ultrastructure of the transition zone between specialized cells (''Flugelzellen'') of Huxley's layer of the inner root sheath and cells of the outer root sheath of the human hair follicle. *Am J Dermatopathol* 13:264–70

Cotsarelis G, Sun TT, Lavker RM (1990) Label-retaining cells reside in the bulge area of pilosebaceous unit: implications for follicular stem cells, hair cycle, and skin carcinogenesis. *Cell* 61:1329–37

Cotsarelis G (2006) Epithelial stem cells: a folliculocentric view. *J Invest Dermatol* 126:1459–68

Coulombe PA, Wong P (2004) Cytoplasmic intermediate filaments revealed as dynamic and multipurpose scaffolds. *Nat Cell Biol* 6:699–706

Dahl PR, Daoud MS, Su WP (1995) Jadassohn–Lewandowski syndrome (pachyonychia congenita). *Semin Dermatol* 14:129–34

De Berker D, Wojnarowska F, Sviland L, Westgate GE, Dawber RPR, Leigh IM (2000) Keratin expression in the normal nail unit: markers of regional differentiation. *Br J Dermatol* 142:89–96

Feinstein A, Friedman J, Schewach M (1988) Pachyonychia congenita. *J Am Acad Dermatol* 19:705–11

Fuchs E, Merrill BJ, Jamora C, DasGupta R (2001) At the roots of a never-ending cycle. *Dev Cell* 1:13–25

Hallman JR, Fang D, Setaluri V, White WL (2002) Microtubule associated protein (MAP-2) expression defines the companion layer of the anagen hair follicle and an analogous zone in the nail unit. *J Cutan Pathol* 29:549–56

Hardy MH (1992) The secret life of the hair follicle. *Trends Genet* 8:55–61

Hashimoto K, Shibazaki S (1976) Ultrastructural study on differentiation and function of hair. In: *Biology and Disease of the Hair*. (Kobori T and Montagna W, eds), University Park Press, Baltimore, 23–57

Hutchin ME, Kariapper MS, Grachtchouk M, Wang A, Wei L, Cummings D *et al.* (2005) Sustained Hedgehog signaling is required for basal cell carcinoma proliferation and survival: conditional skin tumorigenesis recapitulates the hair growth cycle. *Genes Dev* 19:214–23

Ito M (1986) The innermost cell layer of the outer root sheath in anagen hair follicle: light and electron microscopic study. *Arch Dermatol Res* 279:112–9

Ito M (1988) Electron microscopic study on cell differentiation in anagen hair follicles in mice. *J Invest Dermatol* 90:65–72

Ito M (1989) Biologic roles of the innermost cell layer of the outer root sheath in human anagen hair follicle: further electron microscopic study. *Arch Dermatol Res* 281:254–9

Ito M, Kizawa K, Hamada K, Cotsarelis G (2004) Hair follicle stem cells in the lower bulge form the secondary germ, a biochemically distinct but functionally equivalent progenitor cell population, at the termination of catagen. *Differentiation* 72:548–57

Ito M, Liu Y, Yang Z, Nguyen J, Liang F, Morris RJ *et al.* (2005) Stem cells in the hair follicle bulge contribute to wound repair but not to homeostasis of the epidermis. *Nat Med* 11:1351–4

Jensen PJ, Yang T, Yu DW, Baker MS, Risse B, Sun TT *et al.* (2000) Serpins in the human hair follicle. *J Invest Dermatol* 114:917–22

Kaufman CK, Zhou P, Pasolli HA, Rendl M, Bolotin D, Lim KC *et al.* (2003) GATA-3: an unexpected regulator of cell lineage determination in skin. *Genes Dev* 17:2108–22

Kim S, Wong P, Coulombe PA (2006) A keratin cytoskeletal protein regulates protein synthesis and epithelial cell growth. *Nature* 441:362–5

Koch PJ, Mahoney MG, Cotsarelis G, Rothenberger K, Lavker RM, Stanley JR (1998) Desmoglein 3 anchors telogen hair in the follicle. *J Cell Sci* 111:2529–37

Langbein L, Rogers MA, Praetzel S, Aoki N, Winter H, Schweizer J (2002) A novel epithelial keratin, hK6irs1, is expressed differentially in all layers of the inner root sheath, including specialized huxley cells (Flugelzellen) of the human hair follicle. *J Invest Dermatol* 118:789–99

Langbein L, Rogers MA, Praetzel S, Winter H, Schweizer J (2003) K6irs1, K6irs2, K6irs3, and K6irs4 represent the inner-root-sheath-specific type II epithelial keratins of the human hair follicle. *J Invest Dermatol* 120:512–22

Langbein L, Schweizer J (2005) Keratins of the human hair follicle. *Int Rev Cytol* 243:1–78

Levy V, Lindon C, Harfe BD, Morgan BA (2005) Distinct stem cell populations regenerate the follicle and interfollicular epidermis. *Dev Cell* 9:855–61

Li Y, Rosen JM (2005) Stem/progenitor cells in mouse mammary gland development and breast cancer. *J Mammary Gland Biol Neoplasia* 10:17–24

Lin MT, Levy ML, Bowden PE, Magro C, Baden L, Baden HP *et al.* (1999) Identification of sporadic mutations in the helix initiation motif of keratin 6 in two pachyonychia congenita patients: further evidence for a mutational hot spot. *Exp Dermatol* 8:115–9

Liu Y, Lyle S, Yang Z, Cotsarelis G (2003) Keratin 15 promoter targets putative epithelial stem cells in the hair follicle bulge. *J Invest Dermatol* 121:963–8

Lu H, Hesse M, Peters B, Magin TM (2005) Type II keratins precede type I keratins during early embryonic development. *Eur J Cell Biol* 84:709–18

Lyle S, Christofidou-Solomidou M, Liu Y, Elder DE, Albelda S, Cotsarelis G (1998) The C8/144B monoclonal antibody recognizes cytokeratin 15 and defines the location of human hair follicle stem cells. *J Cell Sci* 111(Part 21):3179–88

McGowan KM, Coulombe PA (1998) The wound repair associated keratins 6, 16, and 17: Insights into the role of intermediate filaments in specifying cytoarchitecture. In: *Subcellular Biochemistry: Intermediate Filaments*. (Harris JR, Herrmann, H, eds), London: Plenum Publishing Co, 141–65

McGowan KM, Coulombe PA (2000) Keratin 17 expression in the hard epithelial context of the hair and nail, and its relevance for the pachyonychia congenita phenotype. *J Invest Dermatol* 114:1101–7

McGowan KM, Tong X, Colucci-Guyon E, Langa F, Babinet C, Coulombe PA (2002) Keratin 17 null mice exhibit age- and strain-dependent alopecia. *Genes Dev* 16:1412–22

McLean WHI, Rugg EL, Lunny DP, Morley SM, Lane EB, Swensson O *et al.* (1995) Keratin 16 and keratin 17 mutations cause pachyonychia congenita. *Nat Genet* 9:273–8

Michel M, Torok N, Godbout MJ, Lussier M, Gaudreau P, Royal A *et al.* (1996) Keratin 19 as a biochemical marker of skin stem cells *in vivo* and *in vitro*: keratin 19 expressing cells are differentially localized in function of anatomic sites, and their number varies with donor age and culture stage. *J Cell Sci* 109:1017–28

Millar SE (2002) Molecular mechanisms regulating hair follicle development. *J Invest Dermatol* 118:216–25

Morris RJ, Fischer SM, Slaga TJ (1986) Evidence that a slowly cycling subpopulation of adult murine epidermal cells retains carcinogen. *Cancer Res* 46:3061–6

Morris RJ, Liu Y, Marles L, Yang Z, Trempus C, Li S *et al.* (2004) Capturing and profiling adult hair follicle stem cells. *Nat Biotechnol* 22:411–7

Muller-Rover S, Handjiski B, van der Veen C, Eichmuller S, Foitzik K, McKay IA *et al.* (2001) A comprehensive guide for the accurate classification of murine hair follicles in distinct hair cycle stages. *J Invest Dermatol* 117:3–15

Nachat R, Mechin MC, Charveron M, Serre G, Constans J, Simon M (2005) Peptidylarginine deiminase isoforms are differentially expressed in the anagen hair follicles and other human skin appendages. *J Invest Dermatol* 125:34–41

O'Guin WM, Sun TT, Manabe M (1992) Interaction of trichohyalin with intermediate filaments: three immunologically defined stages of trichohyalin maturation. *J Invest Dermatol* 98:24–32

Oshima H, Rochat A, Kedzia C, Kobayashi K, Barrandon Y (2001) Morphogenesis and renewal of hair follicles from adult multipotent stem cells. *Cell* 104:233–45

Ohyama M, Terunuma A, Tock CL, Radonovich MF, Pise-Masison CA, Hopping SB *et al.* (2006) Characterization and isolation of stem cell-enriched human hair follicle bulge cells. *J Clin Invest* 116:249–60

Paladini RD, Coulombe PA (1999) The functional diversity of epidermal keratins revealed by the partial rescue of the keratin 14 null phenotype by keratin 16. *J Cell Biol* 146:1185–201

Paus R, Cotsarelis G (1999) The biology of hair follicles. *N Engl J Med* 341:491–7

Paus R, Muller-Rover S, Van Der Veen C, Maurer M, Eichmuller S, Ling G *et al.* (1999) A comprehensive guide for the recognition and classification of distinct stages of hair follicle morphogenesis. *J Invest Dermatol* 113:523–32

Poblet E, Jimenez F, de Cabo C, Prieto-Martin A, Sanchez-Prieto R (2005) The calcium-binding protein calretinin is a marker of the companion cell layer of the human hair follicle. *Br J Dermatol* 152:1316–20

Porter RM, Corden LD, Lunny DP, Smith FJ, Lane EB, McLean WH (2001) Keratin K6irs is specific to the inner root sheath of hair follicles in mice and humans. *Br J Dermatol* 145:558–68

Rothnagel JA, Roop D (1995) Hair follicle companion layer: reacquainting an old friend. *J Invest Dermatol* 104:42s–3s

Rothnagel JA, Seki T, Ogo M, Longley MA, Wojcik SM, Rundman DS, Bickenbach JR *et al.* (1999) The mouse keratin 6 isoforms are differentially expressed in the hair follicle, footpad, tongue, and activated epidermis. *Differentiation* 65:119–30

Schweizer J, Marks F (1977) A developmental study of the distribution and frequency of Langerhans cells in relation to formation of patterning in mouse tail epidermis. *J Invest Dermatol* 69:198–204

Schweizer J, Bowden PE, Coulombe PA, Langbein L, Lane EB, Magin TM *et al.* (2006) New consensus nomenclature for mammalian keratins. *J Cell Biol* 174:169–74

Smith FJ, Jonkman MF, van Goor H, Coleman CM, Covello SP, Uitto J *et al.* (1998) A mutation in human keratin K6b produces a phenocopy of the K17 disorder pachyonychia congenita type 2. *Hum Mol Genet* 7:1143–8

Smith FJ, McKenna KE, Irvine AD, Bingham EA, Coleman CM, Uitto J *et al.* (1999) A mutation detection strategy for the human keratin 6A gene and novel missense mutations in two cases of pachyonychia congenita type 1. *Exp Dermat* 8:109–14

Smith GH, Chepko G (2001) Mammary epithelial stem cells. *Microsc Res Tech* 52:190–203

Smyth I, Ellis T, Hetherington R, Riley E, Narang M, Mahony D *et al.* (2004) Krt6a-Cre transgenic mice direct LoxP-mediated recombination to the companion cell layer of the hair follicle and following induction by retinoic acid to the interfollicular epidermis. *J Invest Dermatol* 122:232–4

Stenback F (1980) Adnexal participation in formation of cutaneous tumors following topical application of 9,10-dimethyl-benzanthracene. *J Cutan Pathol* 7:277–94

Sundberg JP, Hogan ME (1994) Hair types and subtypes in the laboratory mouse. In: *Handbook of Mouse Mutations with Skin and Hair Abnormalities.* (Sunberg JP ed), Boca Raton: CRC Press, 57–68

Takahashi K, Coulombe PA (1996) A transgenic mouse model with an inducible skin blistering disease phenotype. *Proc Natl Acad Sci USA* 93:14776–81

Takahashi K, Coulombe PA (1997) Defining a region of the human keratin 6a gene that confers inducible expression in stratified epithelia of transgenic mice. *J Biol Chem* 272:11979–85

Takahashi K, Paladini R, Coulombe PA (1995) Cloning and characterization of multiple human genes and cDNAs encoding highly related type II keratin 6 isoforms. *J Biol Chem* 270:18581–92

Takahashi K, Yan B, Yamanishi K, Imamura S, Coulombe PA (1998) The two functional keratin 6 genes of mouse are differentially regulated and evolved independently from their human orthologs. *Genomics* 53:170–83

Taylor G, Lehrer MS, Jensen PJ, Sun TT, Lavker RM (2000) Involvement of follicular stem cells in forming not only the follicle but also the epidermis. *Cell* 102:451–61

Templeton SF, Wiegand SE (1997) Pachyonychia congenita-associated alopecia. A microscopic analysis using transverse section technique. *Am J Dermatopathol* 19:180–4

Terrinoni A, Smith FJ, Didona B, Canzona F, Paradisi M, Huber M *et al.* (2001) Novel and recurrent mutations in the genes encoding keratins K6a, K16 and K17 in 13 cases of pachyonychia congenita. *J Invest Dermatol* 117:1391–6

Trempus CS, Morris RJ, Bortner CD, Cotsarelis G, Faircloth RS, Reece JM *et al.* (2003) Enrichment for living murine keratinocytes from the hair follicle bulge with the cell surface marker CD34. *J Invest Dermatol* 120:501–11

Tumbar T, Guasch G, Greco V, Blanpain C, Lowry WE, Rendl M, Fuchs E (2004) Defining the epithelial stem cell niche in skin. *Science* 303:359–63

Wang Z, Wong P, Langbein L, Schweizer J, Coulombe PA (2003) Type II epithelial keratin 6hf (K6hf) is expressed in the companion layer, matrix, and medulla in anagen-stage hair follicles. *J Invest Dermatol* 121: 1276–82

Ward KM, Cook-Bolden FE, Christiano AM, Celebi JT (2003) Identification of a recurrent mutation in keratin 6a in a patient with overlapping clinical features of pachyonychia congenita types 1 and 2. *Clin Exp Dermatol* 28:434–6

Wilson C, Cotsarelis G, Wei ZG, Fryer E, Margolis-Fryer J, Ostead M *et al.* (1994) Cells within the bulge region of mouse hair follicle transiently proliferate during early anagen: heterogeneity and functional differences of various hair cycles. *Differentiation* 55:127–36

Winter H, Langbein L, Praetzel S, Jacobs M, Rogers MA, Leigh IM *et al.* (1998) A novel human type II cytokeratin, K6hf, specifically expressed in the companion layer of the hair follicle. *J Invest Dermatol* 111:955–62

Winter H, Schissel D, Parry DA, Smith TA, Liovic M, Birgitte Lane E *et al.* (2004) An unusual Ala12Thr polymorphism in the 1A alpha-helical segment of the companion layer-specific keratin K6hf: evidence for a risk factor in the etiology of the common hair disorder pseudofolliculitis barbae. *J Invest Dermatol* 122:652–7

Wojcik SM, Imakado S, Seki T, Longley MA, Petherbridge L, Bundman DS *et al.* (1999) Expression of MK6a dominant-negative and C-terminal mutant transgenes in mice has distinct phenotypic consequences in the epidermis and hair follicle. *Differentiation* 65:97–112

Wojcik SM, Longley MA, Roop DR (2001) Discovery of a novel murine keratin 6 (K6) isoform explains the absence of hair and nail defects in mice deficient for K6a and K6b. *J Cell Biol* 154:619–30

Wong P, Colucci-Guyon E, Takahashi K, Gu C, Babinet C, Coulombe PA (2000) Introducing a null mutation in the mouse K6alpha and K6beta genes reveals their essential structural role in the oral mucosa. *J Cell Biol* 150:921–8

Wong P, Coulombe PA (2003) Loss of keratin 6 (K6) proteins reveals a function for intermediate filaments during wound repair. *J Cell Biol* 163:327–37

Wong P, Domergue R, Coulombe PA (2005) Overcoming functional redundancy to elicit pachyonychia congenita-like nail lesions in transgenic mice. *Mol Cell Biol* 25:197–205